

Intracellular colocalization and interaction of IGF-binding protein-2 with the cyclin-dependent kinase inhibitor p21^{CIP1/WAF1} during growth inhibition

Xavier TERRIEN, Elise BONVIN, Sophie CORROYER, Olivier TABARY, Annick CLEMENT and Alexandra HENRION CAUDE¹

INSERM U719, Université Pierre et Marie Curie, Hôpital St-Antoine, 75571 Paris Cedex 12, France

It is presently unknown whether any member of the IGFBP (insulin-like growth factor binding protein) family directly participates in the control of cell proliferation. We have previously documented that induction of IGFBP-2 was associated with inhibition of DNA synthesis in lung alveolar epithelial cells. In the present study, we investigated the relationship between IGFBP-2 and the cell cycle inhibitor p21^{CIP1/WAF1} further. We used serum deprivation to inhibit the proliferation of MLE (mouse lung epithelial)-12 cells, and characterized the spatial localization of IGFBP-2. We found that growth inhibition, which was supported by the strong induction of p21^{CIP1/WAF1}, was correlated with increased secretion of IGFBP-2 and, unexpectedly, with its increased localization in the nucleus and particularly in the cytoplasm. By coimmunoprecipitation, we discovered that IGFBP-2 is capable of binding to p21^{CIP1/WAF1}. Interaction between these

two proteins was further supported by colocalization of the proteins within growth-arrested cells, as visualized by confocal microscopy. Furthermore, this interaction increased with the duration of the stress, but was suppressed when proliferation was restimulated by the addition of serum. The recombinant expression of GFP (green fluorescent protein)-tagged IGFBP-2 in transfected MLE-12 cells demonstrated its ability to bind specifically to p21^{CIP1/WAF1}. Taken together, these results provide a link between IGFBP-2 and p21^{CIP1/WAF1} in the regulation of alveolar lung cell proliferation.

Key words: alveolar epithelium, cell cycle, insulin-like growth factor binding protein-2 (IGFBP-2), lung, p21^{CIP1/WAF1}, protein complex.

INTRODUCTION

IGF-I (insulin-like growth factor-I) and -II, their receptors, and their binding proteins [IGFBP-1 (IGF-binding protein-1) to -6] play important roles in regulating cellular proliferation and transformation, and apoptosis [1]. Based on the high affinities of IGFs for IGFBPs, which exceeds the affinity for their receptors, IGFBPs have long been viewed as carrier proteins that modulate IGF availability and function. This concept has evolved further with studies on the IGF-independent actions of IGFBP-3 and IGFBP-5 in different cell systems. The intrinsic biological activities of IGFBP-3 and -5 were well exemplified by observation of their nuclear targeting and by the identification of nuclear binding partners [2,3]. We provided the first evidence of the nuclear localization of IGFBP-2 within the nuclei of adenocarcinoma cells [4]. Consistent with this, Hoeflich et al. recently studied IGFBP-2 expression *in vivo* and revealed its presence in the intracellular compartment of pancreas, stomach, and brain tissues from transgenic mice overexpressing IGFBP-2 [5]. However, the role and the mechanism of action of IGFBP-2 remains largely unknown.

Paradoxical and conflicting biological effects of IGFBP-2 have been reported. Depending on the context, the effects of increased levels of IGFBP-2 on cell proliferation have been identified as being either positive or negative [6]. Under normal physiological conditions, IGFBP-2 is mainly expressed in foetal tissues and its expression pattern in the lung, in the mesenchyme and in the epithelium appears to correlate positively with phasic changes in lung cell proliferation rates [7]. In addition, mice deficient in IGFBP-2 display normal development [8], although overexpres-

sion of IGFBP-2 in transgenic mice results in reduced body weight, which suggests a negative role for IGFBP-2 in somatic growth [9]. Under pathological or nonphysiological conditions, such as trauma, certain tumours, or during starvation, serum levels of IGFBP-2 are found to be elevated [6]. In particular, a positive correlation between the tumour grade and the level of expression of IGFBP-2 has been described for many tumours [10,11]. Also, studies have indicated that IGFBP-2 increases the tumorigenic potential and mitogenesis of some cancer cells [12–14]. A significant illustration of the complexity of IGFBP-2 is its conflicting role in suppressing the growth of normal prostate epithelial cells, while enhancing the growth of prostate cancer cells [15]. Together, these findings suggest that IGFBP-2 possesses multifarious functions, the understanding of which may come from study of the regulation of its expression.

We have previously reported the involvement of IGFBP-2 in the control of proliferation of type 2 alveolar epithelial cells [16]. In particular, blocking of type 2 cell proliferation induced by various conditions such as serum deprivation [16], oxidant exposure [17] or glucocorticoid treatment [18] was found to be associated with increased expression and accumulation of IGFBP-2. Investigation of the mechanisms underlying these arrests in proliferation led us to discover the involvement of the CDK (cyclin-dependent kinase) inhibitor p21^{CIP1/WAF1} (also called WAF1, CAP20, CIP1 and SDI1) in these processes [19]. p21^{CIP1/WAF1} was initially identified as a gene induced in senescent cells [20]. The widely prevailing view is that p21^{CIP1/WAF1} is induced in response to anti-proliferative stimuli and blocks G1/S-phase progression through the inhibition of CDK2 [21]. In addition, several studies have suggested that p21^{CIP1/WAF1} may also play a role in promoting cell

Abbreviations used: BrdU, bromodeoxyuridine; CDK, cyclin-dependent kinase; DTT, dithiothreitol; ECL, enhanced chemiluminescence; FBS, foetal bovine serum; GFP, green fluorescent protein; IGF, insulin-like growth factor; IGFBP, IGF-binding protein; MLE, mouse lung epithelial.

¹ To whom correspondence should be addressed (email caude@st-antoine.inserm.fr).

survival [22–24], transformation [25,26], tumour progression [2] and/or differentiation [27]. As suggested in these studies, different localization of p21^{CIP1/WAF1} to the nucleus or the cytoplasm may explain these versatile functions.

In the present study, we examined the patterns of expression of IGFBP-2 and p21^{CIP1/WAF1} under conditions of growth inhibition. We present direct experimental evidence that IGFBP-2 is not only secreted, but is also induced within the cell, during growth inhibition. Indeed, we show that IGFBP-2 subcellular localization is influenced by cell proliferation. Strikingly, coimmunoprecipitation and confocal microscopy studies indicated that IGFBP-2 is capable of binding to p21^{CIP1/WAF1}. Using recombinant expression of GFP (green fluorescent protein)-tagged IGFBP-2, we were able to demonstrate the specificity of this interaction. Thus the present study demonstrates a link between IGFBP-2 and the regulation of cell proliferation through its interaction with p21^{CIP1/WAF1}.

EXPERIMENTAL

Cell culture

MLE (mouse lung epithelium)-12 cells were obtained from A.T.C.C. (American Type Culture Collection, Rockville, MD, U.S.A.) and routinely cultured in HITES medium (as recommended by the manufacturer) supplemented with 2% (v/v) FBS (foetal bovine serum), penicillin (1000 units/ml) and streptomycin (500 µg/ml) in a humidified atmosphere with 5% CO₂ at 37°C.

Cell proliferation assays

For growth studies, cells were seeded in 24-well plates (3 × 10⁵ cells/ml). One day later, the medium was changed to HITES medium with antibiotics, with or without 2% FBS. At different intervals, adherent cells were trypsinized and the cell number was counted with a haemocytometer. The Trypan Blue exclusion assay was used to determine cell viability. To quantify cell proliferation, DNA synthesis was measured using BrdU (bromodeoxyuridine), which was included in the medium and assayed using the 5-bromo-2'-deoxyuridine Labelling and Detection Kit III (Roche Diagnostics), according to the manufacturer's instructions. Absorbance at 450 nm was measured with the Bio-Rad plate reader (model 450). As indicated by the manufacturer, the absorbance values correlate directly with the amount of DNA synthesis and thereby with the number of proliferating cells in culture.

Construction of GFP-derived expression plasmids and cell transfection studies

The rat IGFBP-2 cDNA was originally amplified and inserted into the cloning vector pCRII-TOPO (Invitrogen, Cergy-Pontoise, France). IGFBP-2 was subcloned in-frame with the C-terminus or the N-terminus of the GFP tag in the pEGFP-N3 or pEGFP-C3 vector respectively (Clontech, B. D. Biosciences, Le Pont de Claix, France). The plasmid pCRII-TOPO-IGFBP-2 was digested with EcoRI to generate a 962 bp fragment, which was inserted into pEGFP-C3 at a unique EcoRI site downstream of the GFP sequence. This plasmid was called pEGFP-C3-IGFBP-2. To generate pEGFP-N3-IGFBP-2, the pCRII-TOPO-IGFBP-2 was used as a template for PCR amplification using the T7 primer and the specific primer 5'-AGTGGATCCGTACTGCACCCCTTG-3', which enabled mutation of the stop codon in the rat IGFBP-2 cDNA and the creation of a restriction site for sub-cloning. The PCR product was digested with BamHI to generate a 1059 bp

fragment which was inserted into pEGFP-N3 at a unique BamHI site upstream of the GFP sequence. In all cases, the orientation of the inserts was confirmed by restriction enzyme analysis and the integrity of constructs was confirmed by sequencing. Expression of the GFP-IGFBP-2 fusion protein was monitored by Western blot analysis of extracts from transfected MLE-12 cells. For transfection, DNA plasmids were prepared by Qiagen HiSpeed Maxiprep (Qiagen, Courtaboeuf, France). MLE-12 cells were seeded at a density of 3 × 10⁵ cells/ml either in 24-well dishes and plated onto glass slides for localization studies, or in 10 cm dishes for Western blot and immunoprecipitation studies. Accordingly, MLE-12 cells were transfected with either 0.8 µg or 24 µg of plasmid DNA with LipofectAMINETM 2000 reagent (Invitrogen, Cergy-Pontoise, France) for 6 h. Transient transfection was carried out according to the manufacturer's instructions, and using either pEGFP-C3-IGFBP-2 or pEGFP-N3-IGFBP-2. Post-transfection, cells were cultured for 24 h in the presence of serum.

Preparation of cell extracts

MLE-12 cells (3 × 10⁵ cells/ml) were seeded on 10 cm plastic dishes and incubated for 24 h in complete medium. They were washed three times with serum-free medium and were then either used for control experiments or made quiescent, where indicated, by serum starvation for 24, 48 or 72 h. At the end of the incubation period, the conditioned medium was collected for ligand-binding blot experiments. For protein extraction, cells were washed with cold PBS, scraped from the dish with a rubber policeman and pelleted by centrifugation at 400 g for 15 min at 4°C. In order to prepare total protein extracts, the cell pellet was lysed on ice by a 1 h incubation with a hypotonic buffer [250 mM NaCl, 50 mM Hepes, 5 mM EDTA, 0.1% Nonidet P40, 500 µM sodium orthovanadate, 5 mM sodium pyrophosphate, 1 mM DTT (dithiothreitol) and protease inhibitor cocktail (Sigma Aldrich, Saint-Quentin Fallavier, France)]. Cell lysates were centrifuged at 15 000 g for 10 min at 4°C. Cytoplasmic protein extracts were prepared according to a modification of the protocol of Schreiber et al. [28]. Briefly, the cell pellet was lysed on ice by a 15 min incubation with buffer A (10 mM Hepes, 10 mM KCl, 1 mM EDTA, 1.5 mM MgCl₂, 1 mM DTT and protease inhibitor cocktail), after which one tenth-volume (1:10, v/v) of a 10% solution of Triton X-100 (Sigma Aldrich, Saint-Quentin Fallavier, France) was added. The homogenate was centrifuged at 15 000 g for 5 min and the supernatant containing the cytoplasmic protein extracts was recovered. For kinase assays, the nuclear pellet was resuspended in ice-cold buffer B (420 mM KCl, 20 mM Hepes, 0.2 mM EDTA, 1.5 mM MgCl₂ and protease inhibitor cocktail), and incubated on ice for 30 min on an orbital shaker. The homogenate was centrifuged at 15 000 g for 30 min at 4°C and the supernatant containing nuclear protein extracts was recovered. In order to prepare crude nuclear extracts for Western blot analysis, the cell pellet was lysed on ice by a 10 min incubation with buffer C (60 mM KCl, 15 mM NaCl, 15 mM Hepes, 2 mM EDTA, 0.5 mM EGTA, 0.15 mM spermine, 0.5 mM spermidine, 2 mM 2-mercaptoethanol, 1 mM PMSF) containing 1.7 M sucrose. Lysates were loaded onto 6 volumes of buffer C containing 2.4 M sucrose, and centrifuged at 25 000 g for 1 h at 4°C. Nuclear pellets were resuspended in buffer D (20 mM Hepes, 25% glycerol, 8.8 mM MgCl₂, 0.2 mM EDTA, 0.15 mM spermine and 0.5 mM spermidine) containing 140 mM NaCl. After incubation on ice for 30 min, one volume of buffer D containing 700 mM NaCl was added. Lysates were incubated on ice for another 30 min and centrifuged at 35 000 g for 30 min at 4°C. The supernatant containing crude nuclear protein extracts was recovered. In each

preparation of cell extracts, protein concentration was determined by the method of Bradford using BSA as standard.

Antibodies and Western blot analysis

Proteins were separated by SDS/PAGE (10%) and transferred onto ImmobilonTM-P membrane (Millipore, Bedford, MA, U.S.A.) for 1 h at 300 mA in transfer buffer [24 mM Tris base, 191 mM glycine and 20% (v/v) methanol]. Membranes were blocked for 1 h at 18–22°C with 5% (w/v) non-fat milk powder in PBST (PBS, 0.1% Tween-20) and incubated overnight at 4°C with primary antibody [anti-IGFBP-2 (Santa Cruz Biotechnology, Le Perray-en-Yvelines, France), 1:600; anti-p21, 1:500; anti-GFP (BD Living Colors), 1:500; anti-cyclin A, 1:500; anti-cyclin E, 1:500; anti- β -actin (Sigma–Aldrich, Saint-Quentin Fallavier, France), 1:1000; anti-TATA-binding protein, 1:500] in the blocking solution. After washing in PBST, blots were incubated for 1 h at 18–22°C in PBST with secondary antibodies coupled to horseradish peroxidase [anti-(goat IgG), 1:5000; anti-(rabbit IgG) or anti-(mouse IgG) (Pierce Chemical Co, Brebières, France), 1:2500]. Immunoblots were incubated with ECL (enhanced chemiluminescence) SuperSignal West Pico solution (Pierce Chemical Co). Densitometric analysis was performed using Multigauge Las 3000 software (Fuji, Paris, France).

Western ligand blotting and immunoblotting

Western ligand blotting was performed according to the method of Hossenlopp et al. [29]. For all conditions, either control or serum-starved MLE-12 cells were cultured for 8 h in fresh serum-free medium before collection of the conditioned medium. Briefly, the conditioned medium from the different cell culture conditions was centrifuged (10000 g for 10 min), desalted on Sephadex G-25 columns (Pharmacia-LKB, Sweden) and lyophilized. Lyophilized supernatants were suspended in 100 mM Tris buffer, pH 7.5. Samples were adjusted to 3×10^5 cells and analysed by SDS/PAGE (10%) under non-reducing conditions. Proteins were transferred to nitrocellulose membranes and probed with a mixture of ¹²⁵I-IGF-I and ¹²⁵I-IGF-II (2×10^5 c.p.m.). The blots were then exposed to X-ray films for 2 weeks at –80°C. After autoradiography, the membranes were incubated with anti-IGFBP-2 antibody overnight at 4°C. After washing in PBST (PBS and 0.1% Tween-20), blots were incubated for 1 h at 18–22°C with a 1:5000 dilution in PBST of peroxidase-conjugated anti-(goat IgG).

Immunoprecipitation and assay of protein kinases

Pre-cleared total protein extracts (0.1 mg) were incubated overnight at 4°C with anti-IGFBP-2, anti-p21^{CIP1/WAF1} or anti-GFP antibody, or non-immune rabbit IgG as a control, after which 30 μ l of Protein A–Sepharose beads (Amersham Biosciences, Orsay, France) was added and incubated for 1 h at 4°C. Immunocomplexes were then pelleted and washed four times with 500 μ l of washing buffer [20 mM Tris/HCl (pH 7.5), 4 mM MgCl₂ and 1 mM DTT]. The samples were then resuspended in SDS sample buffer [62.5 mM Tris/HCl (pH 6.8), 4% SDS, 10% glycerol, 0.025% Bromophenol Blue and 5% 2-mercaptoethanol] and analysed by Western blot as described above. CDK activity was assayed using histone H1 (Boehringer, Mannheim, Germany) as substrate, as described previously [30]. Briefly, nuclear extract (50 μ g) was incubated with Protein A–Sepharose conjugated to anti-cyclin A, anti-CDK2 or anti-cyclin E antibody (see above). The immunoprecipitated kinase activities were assayed for 30 min at 30°C, in a total volume of 25 μ l containing 50 mM Tris/HCl (pH 7.4), 10 mM MgCl₂, 1 mM DTT, 20 μ M ATP, 1 μ Ci of [γ -³²P]ATP (4500 mCi/mmol) (Amersham Biosciences, Orsay,

France) and 5 μ l of 1 mg/ml histone H1. The reaction was stopped with SDS loading buffer. The reacted samples were separated on SDS/PAGE, and kinase activity was detected by autoradiography.

Fluorescence microscopy

All cells were grown on coverslips and fixed with 4% (w/v) paraformaldehyde in PBS for 10 min at room temperature, then permeabilized with 0.075% saponin in PBS containing 1% BSA. Controls included cells incubated with 1% BSA and rabbit IgG or mouse IgG (0.5 g/ml). Three different procedures were performed. First, for the characterization of intracellular IGFBP-2, fixed cells were incubated with a rabbit polyclonal anti-IGFBP-2 antibody (Upstate Biotechnology, Mundolsheim, France). Cells were rinsed in PBS containing 50 mM NH₄Cl before incubation with an FITC-conjugated anti-rabbit antibody (Jackson ImmunoResearch Laboratories) for 1 h at room temperature. Nuclei were stained by incubating the slides at room temperature for 20 min with 1 mg/ml RNase A (Sigma Aldrich, Saint-Quentin Fallavier, France) and then for 9 min with 0.2 μ g/ml propidium iodide in TBS (0.05 M Tris base, 0.15 M NaCl). Secondly, for the visualization of both endogenous IGFBP-2 and p21^{CIP1/WAF1}, cells were incubated with a goat polyclonal anti-IGFBP-2 antibody. The cells were rinsed in PBS containing 50 mM NH₄Cl prior to incubation with a rhodamine-conjugated anti-goat antibody (Molecular Probes, Cergy-Pontoise, France) for 1 h at room temperature. The slides were then incubated with a mouse monoclonal anti-p21^{CIP1/WAF1} antibody which had been labelled with Alexa FluorTM 488 fluorescent dye using the Zenon Mouse IgG Labeling Kit (Molecular Probes, Cergy-Pontoise, France). Thirdly, for the visualization of GFP-tagged IGFBP-2 protein and endogenous p21^{CIP1/WAF1}, transfected cells were incubated with a mouse monoclonal anti-p21^{CIP1/WAF1} antibody which had been labelled with Alexa FluorTM 555 fluorescent dye using the Zenon Mouse IgG Labeling Kit. The slides were examined directly by confocal laser scanning microscopy using a Leica TCS equipped with a DMR inverted microscope and a numerical aperture 63/1.4 oil objective. A krypton/argon mixed gas laser was used to generate two bands: 488 nm for detection of FITC or GFP, and 568 nm for detection of propidium iodide or rhodamine.

Statistical analysis

Each experiment was performed three times or more. Data are expressed as means \pm S.E.M. Statistical analyses were performed using a Student's *t*-test. Significance was assumed at $P < 0.05$.

RESULTS AND DISCUSSION

IGFBP-2 and p21^{CIP1/WAF1} are similarly induced by conditions of serum deprivation

MLE-12 cells have been used as a model system for alveolar epithelial cells by a number of laboratories. To investigate the molecular mechanisms underlying growth inhibition in alveolar epithelium, MLE-12 cells were used as a complementary model to the rat neonatal type 2 cell line [31], which was extensively studied in our previous works [16–19,30,32,33]. We used serum starvation to suppress any interference from exogenous mitogenic signals. We documented the effects of serum deprivation on MLE-12 cell proliferation by culturing exponentially proliferating cells in the presence or absence of 2% FBS for 24, 48 or 72 h. Under these conditions, cellular viability was assessed by manually counting MLE-12 cells using the Trypan Blue exclusion assay. As shown in Figure 1(A), serum deprivation caused no statistically

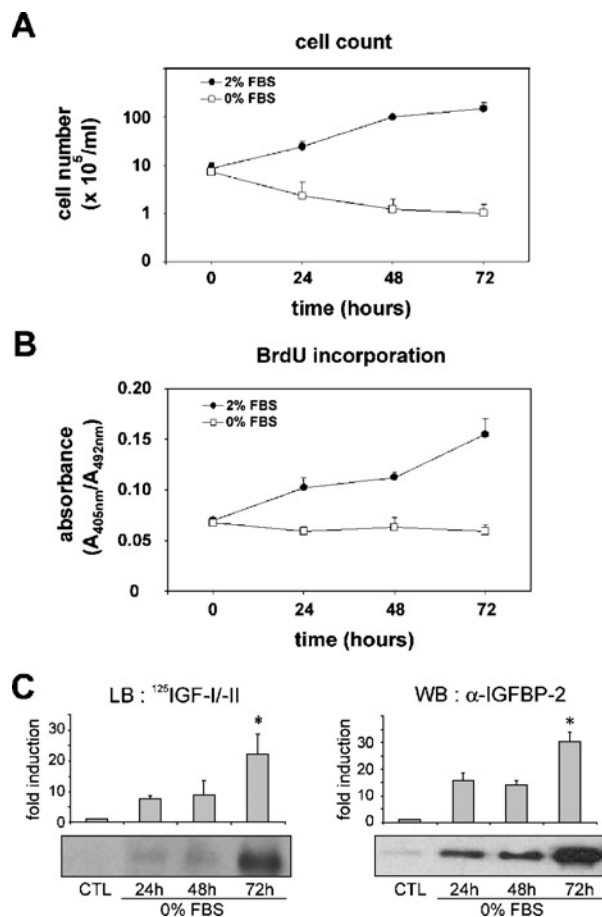


Figure 1 Effect of serum starvation on proliferation of MLE-12 cells and IGFBP-2 secretion

Sub-confluent MLE-12 cells were cultured in HITES medium for 24, 48 or 72 h in the presence (●) or absence (□) of serum. (A) Cell counts were determined per dish using Trypan Blue exclusion assay. (B) DNA synthesis was determined as arbitrary units of absorbance using BrdU incorporation assay. (C) Ligand blot and Western blot analysis of secreted IGFBP-2. Samples from conditioned media corresponding to 3×10^5 cells were desalted, lyophilized, resuspended and analysed by SDS/PAGE. IGFBP-2 capacity for binding IGF was evaluated by Western ligand blotting (LB) by binding with ^{125}I -IGF-I and ^{125}I -IGF-II (left panel). There was a 32 kDa band corresponding to IGFBP-2, which was confirmed by Western blotting (WB) with anti-IGFBP-2 antibody (right panel). Histograms show a quantitative representation obtained from laser densitometric analysis of three independent experiments. Densitometry results were expressed as fold induction. * $P < 0.05$ compared with control (CTL).

significant decrease in cell viability between 0 and 72 h of culture, which indicates that culturing the cells without serum did not result in cell death. The effect of serum deprivation on DNA synthesis was further assessed by BrdU assay (Figure 1B). At each time point of culture, the values obtained without serum were significantly decreased as compared with the values with serum. These results indicate that serum deprivation of MLE-12 cells results in growth inhibition. Moreover, we analysed the IGF-binding capacity of conditioned media by Western ligand blotting and found the induction of a 32 kDa band upon serum starvation, which was further identified as IGFBP-2 by Western immunoblotting (Figure 1C). This induction of secreted IGFBP-2 in serum-deprived MLE-12 cells is consistent with our previous finding in growth-arrested rat alveolar epithelial cells [16–18].

Because the inhibition of proliferation of lung epithelial cells in response to various stresses and in different systems has been shown consistently to coincide with high levels of the CDK

inhibitor $p21^{\text{CIP1/WAF1}}$, we proceeded to characterize its expression. As shown in Figure 2(A), the expression of $p21^{\text{CIP1/WAF1}}$ was strongly induced in the cytoplasm and in the nucleus. At 72 h of serum deprivation, in comparison with control cells, expression of $p21^{\text{CIP1/WAF1}}$ was increased 6.2-fold in the cytoplasm and 4.5-fold in the nucleus. Interestingly, it has been proposed that cytoplasmic localization of $p21^{\text{CIP1/WAF1}}$ may correlate with suppression of cell proliferation in bronchial squamous cell carcinoma [25]. To assess the potential significance of the $p21^{\text{CIP1/WAF1}}$ results, it was important to determine whether the expression or activities of other key cell-cycle regulatory proteins were also modified. Cyclin A and cyclin E were immunoprecipitated with the corresponding antibodies and incubated during *in vitro* kinase assays with purified histone H1 as substrate (Figure 2B). In response to serum deprivation, there was a decrease in the kinase activity associated with cyclin A which was significant at 72 h. By contrast, the kinase activity associated with cyclin E was higher. Interestingly, neither cyclin A nor cyclin E protein levels were significantly altered by the stress (Figure 2C). Thus these results suggest that progression through the S phase in serum-deprived MLE-12 cells is arrested through both induction of $p21^{\text{CIP1/WAF1}}$ and inhibition of the activity of cyclin A-associated complex.

Growth inhibition correlates with increased intracellular localization of IGFBP-2

We and others have provided evidence that IGFBP-2 is located within the cell, in the nuclei of lung adenocarcinoma cells upon oxidant exposure [4], in the peri/nuclear fractions of various tissues isolated from IGFBP-2 transgenic and non-transgenic mice [5], and in the cytoplasm of synovial sarcoma epithelial cells [34]. These findings taken together prompted us to analyse whether conditions of growth inhibition might influence the intracellular localization of IGFBP-2 in MLE-12 cells in response to serum deprivation. Thus we characterized IGFBP-2 expression by Western blotting in the nucleus and in the cytoplasm. Crude nuclear extracts were prepared after isolation of the nuclear fraction from MLE-12 cells by high-density sucrose centrifugation and were monitored by microscopy. The results presented in Figure 3(A) indicate that IGFBP-2 expression was increased in the cytoplasmic and the nuclear fractions in response to serum deprivation. At 72 h of serum deprivation, levels of IGFBP-2 were increased 2.5-fold in the cytoplasm and 1.7-fold in the nucleus, relative to the control.

Based on this finding, we visualized the subcellular localization of IGFBP-2 in growth-inhibited MLE-12 cells by immunofluorescence confocal microscopy. Cells which were permeabilized with saponin were stained with both IGFBP-2 and propidium iodide, and subjected to confocal analysis (Figure 3B). Immunostaining of the cytoplasm and the peri/nuclear compartments by anti-IGFBP-2 antibody was detected in control cells, but was markedly increased with the duration of starvation at 48 and 72 h (Figure 3B). Control experiments performed either without the first antibody or with a non-immune rabbit serum replacing the primary antibody proved that the staining seen was specific for IGFBP-2 (results not shown). The progressive increase in intracellular IGFBP-2 staining with the duration of serum deprivation suggests that IGFBP-2 may be specifically regulated during growth inhibition and that other proteins linked to the cell cycle may be involved in its modulation.

Intracellular IGFBP-2 and $p21^{\text{CIP1/WAF1}}$ interact in growth-inhibited MLE-12 cells

To date, studies which have focused on the relationship between the IGF system and the cell-cycle machinery have consistently

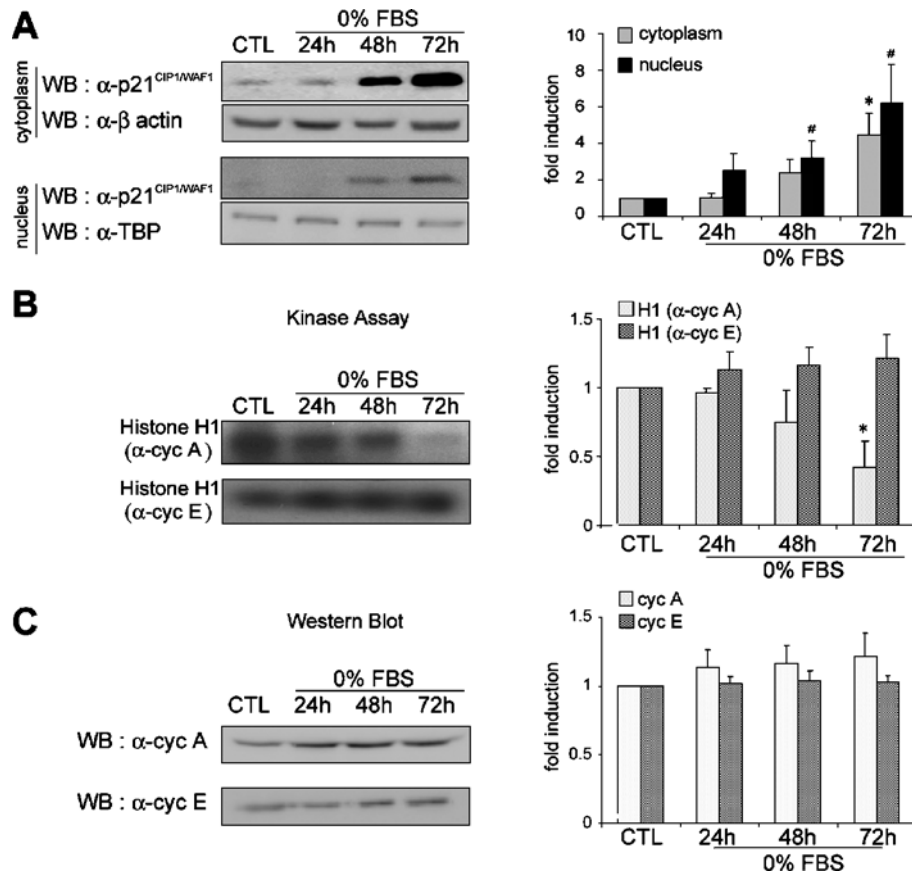


Figure 2 p21^{CIP1/WAF1} expression and CDK activity in growth-inhibited MLE-12 cells

Sub-confluent MLE-12 cells were cultured in HITES medium, in the presence of serum for 24 h (CTL) or in the absence of serum (0% FBS) for 24, 48 or 72 h. **(A)** Western blot (WB) analysis of cytoplasmic and nuclear p21^{CIP1/WAF1} protein. Equal amounts of cytoplasmic and nuclear protein extracts from control cells (CTL) and from serum-deprived cells were analysed by Western blotting with anti-p21^{CIP1/WAF1} antibody. Antibodies against β -actin and TATA-binding protein (α -TBP) were used as controls for protein loading in the cytoplasmic and nuclear extracts respectively. The histogram shows a quantitative representation of cytoplasmic and nuclear levels of p21^{CIP1/WAF1} protein obtained from laser densitometric analysis of three independent experiments. **(B)** CDK activity of cell cycle proteins. Cyclin E and cyclin A were immunoprecipitated and associated kinase activity was assayed using histone H1 as substrate. Equal amounts of nuclear extracts from control cells (CTL) or from serum-deprived cells were used. The histogram shows a quantitative representation obtained from laser densitometric analysis of three independent experiments. **(C)** Western blot analysis of cell cycle proteins. Cyclin E and cyclin A were detected by Western blot analysis with appropriate antisera. Equal amounts of nuclear extracts from control cells (CTL) or from serum-deprived cells were used. The histogram shows a quantitative representation obtained from laser densitometric analysis of three independent experiments. All densitometry results were expressed as fold induction. * and #, $P < 0.05$ compared with control.

identified p21^{CIP1/WAF1} as a critical effector in IGF-mediated signalling in the regulation of proliferation [35], survival [36] or cell death [37]. Here, in order to study the relationship between IGFBP-2 and the control of cell proliferation, we searched for binding partners using various methods such as *in vitro* binding and coimmunoprecipitation, and in particular, tested the ability of IGFBP-2 to associate with p21^{CIP1/WAF1}. Cell lysates from control and serum-deprived cells were immunoprecipitated using a polyclonal anti-IGFBP-2 antibody. Western blot analysis using anti-p21^{CIP1/WAF1} antibody revealed a band after 48 and 72 h, the intensity of which increased with the duration of the stress (Figure 3C). Noticeably, as assessed by also analysing the supernatant fraction of these immunoprecipitates, most p21^{CIP1/WAF1} was efficiently immunoprecipitated by the anti-IGFBP-2 antibody (results not shown). Since this was the first report, to our knowledge, of an intracellular partner for IGFBP-2, we checked the specificity of this binding further by various experiments including reverse coimmunoprecipitation of p21^{CIP1/WAF1}. Cell lysates were thus immunoprecipitated with monoclonal anti-p21^{CIP1/WAF1} antibody, immunoblotted and probed with antibody to IGFBP-2. As shown in Figure 3(C), both

coimmunoprecipitation analyses revealed that IGFBP-2 and p21^{CIP1/WAF1} could be found associated with each other.

This prompted us to test the possibility of colocalization of IGFBP-2 and p21^{CIP1/WAF1} proteins. Thus we studied their intracellular colocalization by immunofluorescence confocal microscopy in cells that had been starved of serum for 72 h. The expression of IGFBP-2 was similar to that of p21^{CIP1/WAF1}, with moderate staining in the nucleus and more intense staining in the cytoplasm, consisting of cytoplasmic aggregates (Figure 3D). This result is consistent with results of Western blot analysis of protein expression (Figures 2A and 3A). The merged images of immunostaining seen through the x -axis and z -axis of optical sections indicated that IGFBP-2 and p21^{CIP1/WAF1} colocalize to a considerable extent (Figure 3D). It is also interesting to note that most, but not all, of the IGFBP-2 was colocalized with p21^{CIP1/WAF1}. The specificity of IGFBP-2 and p21^{CIP1/WAF1} detection was checked by omitting either the anti-IGFBP-2 or the anti-p21^{CIP1/WAF1} antibodies (results not shown). Thus these results indicate that the two proteins IGFBP-2 and p21^{CIP1/WAF1} mainly colocalize in the cytoplasm of lung alveolar MLE-12 cells in response to growth inhibition.

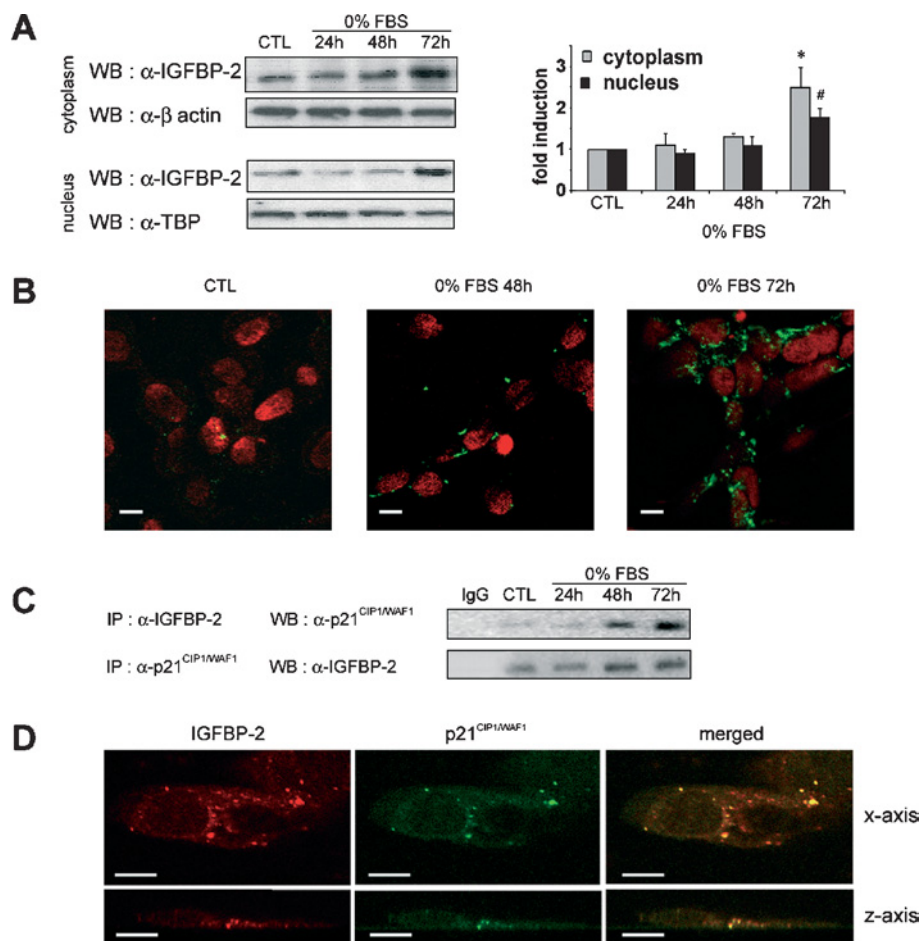


Figure 3 Interaction between intracellular IGFBP-2 and p21^{CIP1/WAF1} during growth inhibition

Sub-confluent MLE-12 cells were cultured in HITES medium, in the presence of serum for 24 h (CTL) or in the absence of serum (0% FBS) for 24, 48 or 72 h. **(A)** Western blot (WB) analysis of cytoplasmic and nuclear IGFBP-2 protein. Equal amounts of cytoplasmic and crude nuclear protein extracts from control cells (CTL) and from serum-deprived cells were analysed by Western blotting with anti-IGFBP-2 antibody. Crude nuclear extracts consisted of cell nuclei that were purified by sucrose density centrifugation, as described in Experimental section. Antibodies against β -actin and TATA-binding protein (α -TBP) were used as controls for protein loading in the cytoplasmic and nuclear extracts respectively. The histogram shows a quantitative representation of cytoplasmic and nuclear levels of IGFBP-2 protein obtained from laser densitometric analysis of three independent experiments. Densitometry results were expressed as fold induction. * and #, $P < 0.05$ compared with control. **(B)** Subcellular localization of IGFBP-2 in proliferating and growth-inhibited MLE-12 cells. Fixed and permeabilized cells were immunostained with primary antibody to IGFBP-2 and secondary FITC-conjugated anti-rabbit antibody. Immunofluorescence staining of IGFBP-2 and nuclei stained with propidium iodide were visualized by confocal microscopy. Scale bars represent 10 μ m. **(C)** Coimmunoprecipitation analysis of the IGFBP-2–p21^{CIP1/WAF1} interaction. Total protein extracts from cultured MLE-12 cells were immunoprecipitated (IP) with anti-IGFBP-2 antibody and p21^{CIP1/WAF1} was detected with anti-p21^{CIP1/WAF1} antibody in the precipitated complex on a Western blot as described in the Experimental section (upper panel). Similarly, p21^{CIP1/WAF1} was immunoprecipitated with anti-p21^{CIP1/WAF1} antibody and Western blotted with anti-IGFBP-2. Representative blots from three independent experiments are shown. **(D)** Subcellular colocalization of IGFBP-2 and p21^{CIP1/WAF1} in growth-inhibited MLE-12 cells. MLE-12 cells were grown for 72 h in the absence of serum. Images of fixed and permeabilized cells were captured by confocal microscopy with respect to both x- (upper panels) and z-axes (lower panels). Cells were immunostained with anti-IGFBP-2 antibody followed by rhodamine-anti-goat IgG secondary antibody (red in left panels). Immunostaining of p21^{CIP1/WAF1} was carried out using anti-p21^{CIP1/WAF1} antibody which had been labelled with Alexa Fluor™ 555 fluorescent dye (green in middle panels). Colocalization of IGFBP-2 and p21^{CIP1/WAF1} was visualized by merging both staining patterns (right panels). Scale bars represent 10 μ m.

Specificity of the interaction between IGFBP-2 and p21^{CIP1/WAF1}

Since it is difficult to determine whether the colocalization of IGFBP-2 and p21^{CIP1/WAF1} is an accurate reflection of events *in vivo*, we next constructed GFP-tagged IGFBP-2. MLE-12 cells were transfected with expression vectors for GFP-tagged IGFBP-2, in parallel with the empty vector acting as a control. It is interesting to note that direct fusion of GFP to either the N-terminus (plasmid pEGFP-N3-IGFBP-2) or the C-terminus (pEGFP-C3-IGFBP-2) of the IGFBP-2 gene product gave similar results. For simplicity, the results reported here used pEGFP-C3-IGFBP-2. To visualize the subcellular localization of the recombinant fusion protein GFP–IGFBP-2, we performed immunofluorescence confocal microscopy on fixed pEGFP-C3-IGFBP-2 transfected cells (Figure 4A). IGFBP-2 was immuno-

stained with a goat anti-IGFBP-2 antibody and a rhodamine-labelled secondary antibody. GFP fusion protein and IGFBP-2 were colocalized into cytoplasmic and peri/nuclear aggregates, confirming both the integrity of the GFP–IGFBP-2 fusion protein and the subcellular localization of IGFBP-2. Using anti-GFP antibody, the expression of cellular GFP fusion protein was then monitored by Western blotting in protein extracts from transfected cells. Figure 4(B) shows a 27 kDa band corresponding to GFP in cells transfected with the empty vector and a 62 kDa band corresponding to GFP–IGFBP-2 in cells transfected with the pEGFP-C3-IGFBP-2 vector.

Coimmunoprecipitation experiments were also performed on MLE-12 cells transfected with pEGFP or pEGFP-C3-IGFBP-2. Cell lysates of untransfected and transfected cells were immunoprecipitated with antibody to the GFP used as a tag, and

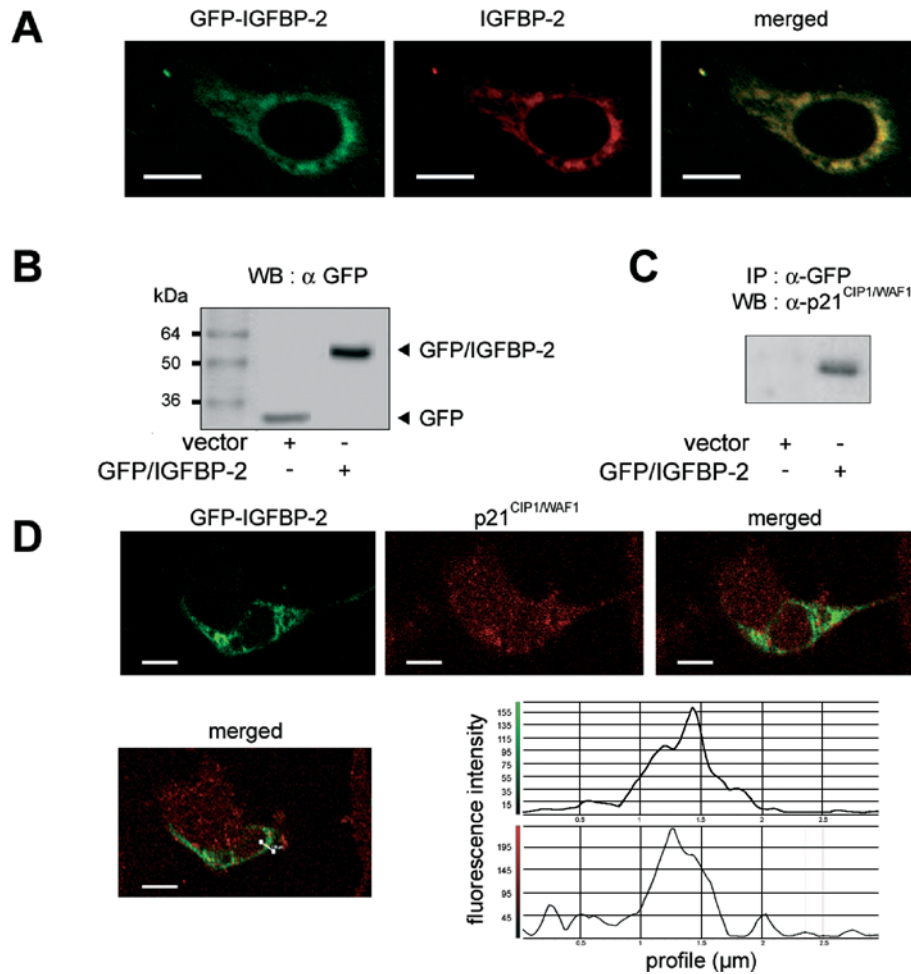


Figure 4 Specific interaction between IGFBP-2 and p21^{CIP1/WAF1} detected by transfection of GFP-IGFBP-2 fusion protein

Sub-confluent MLE-12 cells were transiently transfected with either the empty vector (pEGFP-C3, noted as vector), or the GFP-IGFBP-2 vector (pEGFP-C3-IGFBP-2), and subsequently cultured for 24 h in the presence of serum. **(A)** Dual visualization of GFP-IGFBP-2 fusion protein. Images of fixed cells were taken 24 h post-transfection with pEGFP-C3-IGFBP-2 and show the GFP fluorescence (left panel), and red immunostaining with anti-IGFBP-2 antibody followed by rhodamine-anti-goat IgG secondary antibody (middle panel), together with the merged image (right panel). Scale bars represent 10 μ m. **(B)** Expression of GFP and GFP-IGFBP-2 fusion protein in transfected MLE-12 cells. Equal amounts of total protein extracts from transfected cells were analysed by Western blotting (WB) with monoclonal anti-GFP antibody. GFP protein and GFP-IGFBP-2 fusion protein were detected at the expected sizes of 27 kDa and 62 kDa respectively. **(C)** Coimmunoprecipitation of GFP-IGFBP-2 with endogenous p21^{CIP1/WAF1}. Total protein extracts from MLE-12 cells transfected with the indicated plasmid were immunoprecipitated (IP) with anti-GFP antibody and p21^{CIP1/WAF1} was detected with anti-p21^{CIP1/WAF1} antibody in the precipitated complex on a Western blot as described in the Experimental section. A representative blot from three independent experiments is shown. **(D)** Colocalization of GFP-IGFBP-2 fusion protein and endogenous p21^{CIP1/WAF1} in transfected MLE-12 cells. Images of fixed cells were taken 24 h post-transfection with pEGFP-C3-IGFBP-2 and show the GFP fluorescence (left panel), the red immunostaining with anti-p21^{CIP1/WAF1} antibody, which had been labelled with Alexa FluorTM 555 fluorescent dye (middle panel), together with the merged image (right panel). The profiles of the pixel intensity of the green and red channels along the white line drawn in the merged image show the colocalization of GFP-IGFBP-2 and p21^{CIP1/WAF1}. Scale bars represent 10 μ m.

subjected to Western blotting analysis with antibody to p21^{CIP1/WAF1} as probe. There was no cross-reaction between the anti-GFP antibody and proteins other than the GFP fusion protein in the cell lysate (results not shown). p21^{CIP1/WAF1} could be immunoprecipitated in cells which were transfected with pEGFP-C3-IGFBP-2, but not with the empty vector (Figure 4C).

Furthermore, transfected MLE-12 cells that expressed GFP-IGFBP-2 were immunostained for p21^{CIP1/WAF1} using an anti-p21^{CIP1/WAF1} antibody which had been labelled with Alexa FluorTM 555 fluorescent dye and observed by confocal microscopy. Figure 4(D) shows that GFP-IGFBP-2 and p21^{CIP1/WAF1} colocalized into cytoplasmic aggregates. Thus colocalization and binding of p21^{CIP1/WAF1} and recombinant IGFBP-2 (Figure 4) show consistency with that of p21^{CIP1/WAF1} and endogenous IGFBP-2 (Figure 3).

Interaction between IGFBP-2 and p21^{CIP1/WAF1} is suppressed in cells restimulated with serum

To assess the interaction between IGFBP-2 and p21^{CIP1/WAF1} under conditions of restimulated growth, MLE-12 cells that had been starved of serum for 48 h were re-exposed to serum for another 48 h. Figure 5 shows that addition of serum led MLE-12 cells to re-enter the growth phase, as assessed by an assay for incorporation of BrdU. This was increased 3.4-fold relative to serum-starved cells at 48 h. The interaction between IGFBP-2 and p21^{CIP1/WAF1} was tested by immunoprecipitating cell lysates with either anti-IGFBP-2 antibody (Figure 5) or anti-p21^{CIP1/WAF1} antibody (results not shown). These coimmunoprecipitation experiments resulted in reproducible weak signals in the restimulated condition, indicating low levels of complex when the cells were proliferating.

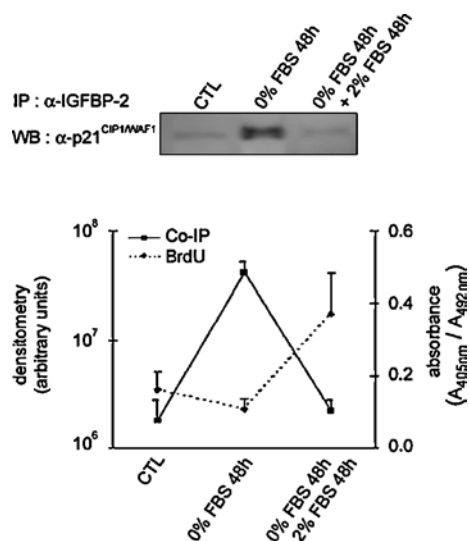


Figure 5 Effect of serum addition to serum-starved MLE-12 cells on proliferation and on the interaction between IGFBP-2 and p21^{CIP1/WAF1}

Sub-confluent MLE-12 cells were seeded and cultured in HITES medium for 24 h in the presence of serum (CTL), then serum-starved for 48 h (0% FBS 48 h), before the addition of serum for 48 h (0% FBS 48 h + 2% FBS 48 h). Total protein extracts from cultured MLE-12 cells were immunoprecipitated (IP) with anti-IGFBP-2 antibody and p21^{CIP1/WAF1} was detected with anti-p21^{CIP1/WAF1} antibody in the precipitated complex on a Western blot (WB). A representative blot is shown above the graph. BrdU incorporation was assayed at the three time points (as outlined in the Experimental section). Densitometry from coimmunoprecipitation experiments and absorbance from BrdU incorporation, each representative of three independent experiments, were plotted as a continuous line and a dashed line respectively.

In fact, the level of interaction between IGFBP-2 and p21^{CIP1/WAF1} was the same in restimulated cells as in the control.

In conclusion, we have identified a spatial colocalization of IGFBP-2 and p21^{CIP1/WAF1} proximal to the nucleus, though this is mainly cytoplasmic. The association of IGFBP-2 and p21^{CIP1/WAF1} was shown by immunoprecipitation of cell extracts with anti-IGFBP-2 as well as anti-p21^{CIP1/WAF1} antibodies. Both the colocalization and the interaction were further confirmed by transfection experiments and fluorescence studies with GFP-tagged IGFBP-2. Whether IGFBP-2 and p21^{CIP1/WAF1} associate in a multiprotein complex, or associate by a direct protein-protein interaction, is not clear and still needs to be addressed. The fact that cytoplasmic localization of IGFBP-2 changes with conditions of growth is a novel concept that warrants specific investigation. In this respect, the characterization of p21^{CIP1/WAF1} as a binding partner in conditions of growth inhibition is highly suggestive of a role of intracellular IGFBP-2 in regulating the cell cycle. We found consistently that the IGFBP-2-p21^{CIP1/WAF1} association was not detected in restimulated MLE-12 cells. In this respect, the cytoplasmic aggregates that were observed by immunofluorescence analysis of both proteins could well be complexes that serve to regulate the cell cycle in concert with proteins of the cytoskeleton, but this is only speculation. Indeed, despite the fact that the described IGFBP-2 binding partners were so far exclusively cell surface proteins [39–41], interaction with the centrosome was reported for IGFBP-4 in primary astrocytes [42], and for p21^{CIP1/WAF1}, through the CIP-1-associated regulator of cyclin B protein [38]. At this time, further studies are required to investigate the role of the complex between IGFBP-2 and p21^{CIP1/WAF1} during inhibition of proliferation.

We especially thank Laurence Perin and Philippe Fontanges for technical assistance. This work was supported by grants from INSERM, Assistance Publique-Hôpitaux de Paris, and the Paris University of Pierre et Marie Curie.

REFERENCES

- Rosenzweig, S. A. (2004) What's new in the IGF-binding proteins? *Growth Horm. IGF Res.* **14**, 329–336
- Lee, S. and Helfman, D. M. (2004) Cytoplasmic p21^{Cip1} is involved in Ras-induced inhibition of the ROCK/LIMK/cofilin pathway. *J. Biol. Chem.* **279**, 1885–1891
- Amaar, Y. G., Thompson, G. R., Linkhart, T. A., Chen, S. T., Baylink, D. J. and Mohan, S. (2002) Insulin-like growth factor-binding protein 5 (IGFBP-5) interacts with a four and a half LIM protein 2 (FHL2). *J. Biol. Chem.* **277**, 12053–12060
- Besnard, V., Corroyer, S., Trugnan, G., Chadelat, K., Nabeyrat, E., Cazals, V. and Clement, A. (2001) Distinct patterns of insulin-like growth factor binding protein (IGFBP)-2 and IGFBP-3 expression in oxidant exposed lung epithelial cells. *Biochim. Biophys. Acta* **1538**, 47–58
- Hoeflich, A., Reisinger, R., Schuett, B. S., Elminger, M. W., Russo, V. C., Vargas, G. A., Jehle, P. M., Lahm, H., Renner-Muller, I. and Wolf, E. (2004) Peri/nuclear localization of intact insulin-like growth factor binding protein-2 and a distinct carboxyl-terminal IGFBP-2 fragment *in vivo*. *Biochem. Biophys. Res. Commun.* **324**, 705–710
- Hoeflich, A., Reisinger, R., Lahm, H., Kiess, W., Blum, W. F., Kolb, H. J., Weber, M. M. and Wolf, E. (2001) Insulin-like growth factor-binding protein 2 in tumorigenesis: protector or promoter? *Cancer Res.* **61**, 8601–8610
- Batchelor, D. C., Hutchins, A. M., Klempf, M. and Skinner, S. J. (1995) Developmental changes in the expression patterns of IGFs, type 1 IGF receptor and IGF-binding proteins-2 and -4 in perinatal rat lung. *J. Mol. Endocrinol.* **15**, 105–115
- Wood, T. L., Rogler, L. E., Czick, M. E., Schuller, A. G. and Pintar, J. E. (2000) Selective alterations in organ sizes in mice with a targeted disruption of the insulin-like growth factor binding protein-2 gene. *Mol. Endocrinol.* **14**, 1472–1482
- Hoeflich, A., Wu, M., Mohan, S., Foll, J., Wanke, R., Froehlich, T., Arnold, G. J., Lahm, H., Kolb, H. J. and Wolf, E. (1999) Overexpression of insulin-like growth factor-binding protein-2 in transgenic mice reduces postnatal body weight gain. *Endocrinology* **140**, 5488–5496
- Reeve, J. G., Schwander, J. and Bleehen, N. M. (1993) IGFBP-2: an important regulator of insulin-like growth factor action in human lung tumours? *Growth Regul.* **3**, 82–84
- Sallinen, S. L., Sallinen, P. K., Haapasalo, H. K., Helin, H. J., Helen, P. T., Schraml, P., Kallioniemi, O. P. and Kononen, J. (2000) Identification of differentially expressed genes in human gliomas by DNA microarray and tissue chip techniques. *Cancer Res.* **60**, 6617–6622
- Menouny, M., Binoux, M. and Babajko, S. (1998) IGFBP-2 expression in a human cell line is associated with increased IGFBP-3 proteolysis, decreased IGFBP-1 expression and increased tumorigenicity. *Int. J. Cancer* **77**, 874–879
- Hoeflich, A., Fettscher, O., Lahm, H., Blum, W. F., Kolb, H. J., Engelhardt, D., Wolf, E. and Weber, M. M. (2000) Overexpression of insulin-like growth factor-binding protein-2 results in increased tumorigenic potential in Y-1 adrenocortical tumor cells. *Cancer Res.* **60**, 834–838
- Slootweg, M. C., Ohlsson, C., Salles, J. P., de Vries, C. P. and Netelenbos, J. C. (1995) Insulin-like growth factor binding proteins-2 and -3 stimulate growth hormone receptor binding and mitogenesis in rat osteosarcoma cells. *Endocrinology* **136**, 4210–4217
- Moore, M. G., Wetterau, L. A., Francis, M. J., Peehl, D. M. and Cohen, P. (2003) Novel stimulatory role for insulin-like growth factor binding protein-2 in prostate cancer cells. *Int. J. Cancer* **105**, 14–19
- Mouhieddine, O. B., Cazals, V., Maitre, B., Le Bouc, Y., Chadelat, K. and Clement, A. (1994) Insulin-like growth factor-II (IGF-II), type 2 IGF receptor, and IGF-binding protein-2 gene expression in rat lung alveolar epithelial cells: relation to proliferation. *Endocrinology* **135**, 83–91
- Cazals, V., Mouhieddine, B., Maitre, B., Le Bouc, Y., Chadelat, K., Brody, J. S. and Clement, A. (1994) Insulin-like growth factors, their binding proteins, and transforming growth factor- β 1 in oxidant-arrested lung alveolar epithelial cells. *J. Biol. Chem.* **269**, 14111–14117
- Mouhieddine, O. B., Cazals, V., Kuto, E., Le Bouc, Y. and Clement, A. (1996) Glucocorticoid-induced growth arrest of lung alveolar epithelial cells is associated with increased production of insulin-like growth factor binding protein-2. *Endocrinology* **137**, 287–295
- Corroyer, S., Nabeyrat, E. and Clement, A. (1997) Involvement of the cell cycle inhibitor CIP1/WAF1 in lung alveolar epithelial cell growth arrest induced by glucocorticoids. *Endocrinology* **138**, 3677–3685

- 20 Noda, A., Ning, Y., Venable, S. F., Pereira-Smith, O. M. and Smith, J. R. (1994) Cloning of senescent cell-derived inhibitors of DNA synthesis using an expression screen. *Exp. Cell Res.* **211**, 90–98
- 21 Sherr, C. J. and Roberts, J. M. (1995) Inhibitors of mammalian G1 cyclin-dependent kinases. *Genes Dev.* **9**, 1149–1163
- 22 Asada, M., Yamada, T., Ichijo, H., Delia, D., Miyazono, K., Fukumuro, K. and Mizutani, S. (1999) Apoptosis inhibitory activity of cytoplasmic p21^{CIP1/WAF1} in monocytic differentiation. *EMBO J.* **18**, 1223–1234
- 23 Gorospe, M., Wang, X. and Holbrook, N. J. (1999) Functional role of p21 during the cellular response to stress. *Gene Expr.* **7**, 377–385
- 24 Dotto, G. P. (2000) p21^{WAF1/CIP1}: more than a break to the cell cycle? *Biochim. Biophys. Acta* **1471**, 43–56
- 25 Hirano, T., Kakihana, M., Tsuji, K., Shibamura, H., Ohira, T., Ikeda, N., Kawate, N., Konaka, C., Ebihara, Y. and Kato, H. (1999) The relationship between p21^{WAF1} expression patterns and cell proliferation during the tumorigenesis of the bronchus. *Int. J. Oncol.* **15**, 253–258
- 26 Zhou, B. P., Liao, Y., Xia, W., Spohn, B., Lee, M. H. and Hung, M. C. (2001) Cytoplasmic localization of p21^{Cip1/WAF1} by Akt-induced phosphorylation in HER-2/neu-overexpressing cells. *Nat. Cell Biol.* **3**, 245–252
- 27 Tanaka, H., Yamashita, T., Asada, M., Mizutani, S., Yoshikawa, H. and Tohyama, M. (2002) Cytoplasmic p21^{CIP1/WAF1} regulates neurite remodeling by inhibiting Rho-kinase activity. *J. Cell Biol.* **158**, 321–329
- 28 Schreiber, E., Matthias, P., Muller, M. M. and Schaffner, W. (1989) Rapid detection of octamer binding proteins with 'mini-extracts', prepared from a small number of cells. *Nucleic Acids Res.* **17**, 6419
- 29 Hossenlopp, P., Seurin, D., Segovia-Quinson, B., Hardouin, S. and Binoux, M. (1986) Analysis of serum insulin-like growth factor binding proteins using western blotting: use of the method for titration of the binding proteins and competitive binding studies. *Anal. Biochem.* **154**, 138–143
- 30 Nabeyrat, E., Corroyer, S., Epaud, R., Besnard, V., Cazals, V. and Clement, A. (2000) Retinoic acid-induced proliferation of lung alveolar epithelial cells is linked to p21^{CIP1} downregulation. *Am. J. Physiol. Lung Cell Mol. Physiol.* **278**, L42–L50
- 31 Clement, A., Steele, M. P., Brody, J. S. and Riedel, N. (1991) SV40T-immortalized lung alveolar epithelial cells display post-transcriptional regulation of proliferation-related genes. *Exp. Cell Res.* **196**, 198–205
- 32 Nabeyrat, E., Besnard, V., Corroyer, S., Cazals, V. and Clement, A. (1998) Retinoic acid-induced proliferation of lung alveolar epithelial cells: relation with the IGF system. *Am. J. Physiol.* **275**, L71–L79
- 33 Nabeyrat, E., Corroyer, S., Besnard, V., Cazals-Laville, V., Bourbon, J. and Clement, A. (2001) Retinoic acid protects against hyperoxia-mediated cell-cycle arrest of lung alveolar epithelial cells by preserving late G1 cyclin activities. *Am. J. Respir. Cell Mol. Biol.* **25**, 507–514
- 34 Allander, S. V., Illei, P. B., Chen, Y., Antonescu, C. R., Bittner, M., Ladanyi, M. and Meltzer, P. S. (2002) Expression profiling of synovial sarcoma by cDNA microarrays: association of ERBB2, IGFBP2, and ELF3 with epithelial differentiation. *Am. J. Pathol.* **161**, 1587–1595
- 35 Dupont, J., Karas, M. and LeRoith, D. (2003) The cyclin-dependent kinase inhibitor p21^{CIP1/WAF1} is a positive regulator of insulin-like growth factor I-induced cell proliferation in MCF-7 human breast cancer cells. *J. Biol. Chem.* **278**, 37256–37264
- 36 Lawlor, M. A. and Rotwein, P. (2000) Insulin-like growth factor-mediated muscle cell survival: central roles for Akt and cyclin-dependent kinase inhibitor p21. *Mol. Cell. Biol.* **20**, 8983–8995
- 37 Murray, S. A., Zheng, H., Gu, L. and Jim Xiao, Z. X. (2003) IGF-1 activates p21 to inhibit UV-induced cell death. *Oncogene* **22**, 1703–1711
- 38 McShea, A., Samuel, T., Eppel, J. T., Galloway, D. A. and Funk, J. O. (2000) Identification of CIP-1-associated regulator of cyclin B (CARB), a novel p21-binding protein acting in the G2 phase of the cell cycle. *J. Biol. Chem.* **275**, 23181–23186
- 39 Schutt, B. S., Langkamp, M., Rauschnabel, U., Ranke, M. B. and Emlinger, M. W. (2004) Integrin-mediated action of insulin-like growth factor binding protein-2 in tumor cells. *J. Mol. Endocrinol.* **32**, 859–868
- 40 Pereira, J. J., Meyer, T., Docherty, S. E., Reid, H. H., Marshall, J., Thompson, E. W., Rossjohn, J. and Price, J. T. (2004) Bimolecular interaction of insulin-like growth factor (IGF) binding protein-2 with $\alpha v \beta 3$ negatively modulates IGF-I-mediated migration and tumor growth. *Cancer Res.* **64**, 977–984
- 41 Song, S. W., Fuller, G. N., Khan, A., Kong, S., Shen, W., Taylor, E., Ramdas, L., Lang, F. F. and Zhang, W. (2003) Iip45, an insulin-like growth factor binding protein 2 (IGFBP-2) binding protein, antagonizes IGFBP-2 stimulation of glioma cell invasion. *Proc. Natl. Acad. Sci. U.S.A.* **100**, 13970–13975
- 42 Chesik, D., Wilczak, N. and De Keyser, J. (2004) Insulin-like growth factor binding protein-4 interacts with centrosomes and microtubules in primary astrocytes. *Neuroscience* **125**, 381–390